Prediction of grinding residual stresses

D. Nélias, V. Boucly

LaMCoS, INSA-Lyon, CNRS UMR5259, F69621, France
URL: *www.insa-lyon.fr* ***e-mail*** *: daniel.nelias@insa-lyon.fr, vincent.boucly@insa-lyon.fr*

ABSTRACT: Residual stresses due to machining are the results of the thermo-mechanical history of the piece/tool interface. The magnitude and the gradient of stress play a key role for the surface integrity. A thermo-mechanical model has been developed. It allows simulating the rolling/sliding contact between an elastic tool in rotation along its own axis and an elastic-plastic flat in translation. The analysis includes the effects of both the normal and tangential loading. Frictional heating is also considered. The model is based on a semi-analytical method and the transient 3D contact problem is fully solved. Compared to the finite element method the computing time is reduced by several orders of magnitude. This technique has already been successfully applied to the simulation of running-in and wear, and to fretting wear, and a first attempt to simulate residual stress and strain due to the contact between a grinding tool and a work piece is made here. First results are presented for various stationary and transient thermo-mechanical loading histories.

Key words: residual stress, grinding, 3D contact, elastic-plastic, semi-analytical method

1 INTRODUCTION

The knowledge of residual stresses due to surface finishing is of prime importance both for the manufacturer that should monitor the process and for the end user who will include the initial stress state in the fatigue life calculation. A better understanding of the physics involved will permit to optimize the process for a given application. An integral method, also called the semi-analytical method (SAM), is used here to model the contact between the grinding tool and the work piece. This analyze allows to investigate separately mechanical (normal and tangential loading) and thermal (moving heat source) effects.
The contact problem is solved by the numerical summation of analytical solutions of elementary problems, such as the effect of a cuboid of uniform plastic strain in a half-space. Analytical solutions are based on the assumptions of half-space and small strains and displacements, which fit well contact problems where the contact area is small compared to the length of the bodies. The use of a uniform mesh along each direction allows speeding the computation through the discrete-convolution fast fourier transform (DC-FFT). It is then possible to get a 3D solution in a CPU time comparable to 2D problem when solved by FEM.
The model is based on the pioneering theoretical and numerical work of Jacq et al. [1] who introduced plasticity in 3D contact solver, and on the work of Liu and Wang [2] for thermal effects. These 2 approaches have been recently coupled by Boucly et al. [3], and the numerical procedures optimized both by the use of the conjugate gradient method (CGM) to solve the contact problem [4] and by the implementation of a return-mapping algorithm for the plasticity loop [5,6]. Note that the analytical relations that give the normal displacement of a surface point and the subsurface residual stresses due to a plastic cuboid are given by Chiu [7,8].
To the authors knowledge this is the first time that this technique is used to predict residual stresses due to grinding. This technique has already been successfully applied to the simulation of running-in and wear [6], fretting wear [9], the rolling of an elastic ellipsoid on an elastic-plastic flat [10] and the rolling of an elastic sphere on a surface dent [11].
The methodology presented here is different from conventional approaches based on FEM, mostly 2D in plane strain, see for example [12-13].

2 THERMAL-ELASTIC-PLASTIC CONTACT MODEL

2.1 Elastic contact

The contact problem consists of solving the following set of equations:

$$\sum_{(k,l)\in I_g} K_{i-k,j-l}\, p_{kl} = h_{ij} + \alpha, \quad (i,j)\in I_c \qquad (1a)$$

$$p_{ij} > 0, \quad (i,j) \in I_c; \tag{1b}$$

$$\sum_{(k,l)\in I_g} K_{i-k,j-l} p_{kl} \geq h_{ij} + \alpha, \quad (i,j) \notin I_c; \tag{1c}$$

$$p_{ij} = 0, \quad (i,j) \notin I_c; \tag{1d}$$

$$a_x a_y \sum_{(i,j)\in I_g} p_{ij} = P_0. \tag{1e}$$

where α is the rigid body displacement, a_x and a_y are the discretization steps along the x and y directions, respectively, P_0 the total normal load, h_{ij} the gap between the surfaces and Ic the contact area.

2.2 Solving the contact problem

The conjugate gradient method (CGM) and the discrete convolution fast Fourier transforms (DC-FFT) are used to solve the contact problem. The contact could be either load (the rigid body displacement α is then an unknown) or displacement (then the normal load P becomes unknown in the set of eq. 1) driven. The algorithm is given by Polonsky and Keer [4] for the load driven problem and by Boucly et al. [14] for the displacement driven one.

2.3 Introduction of thermal and plastic effects

The thermal-elastic contact solver is one of the modules of the thermal-elastic-plastic code, called Plastkid®. For more details the reader can refer to Jacq et al. [1] and Boucly et al. [3]. A return-mapping algorithm with an elastic predictor and a plastic corrector along with the von Mises criterion has been implemented [6]. Theses numerical techniques allow to speed up very significantly the convergence speed.

From an initial state (geometry, plastic strain and hardening state at each point) and by imposing either the normal load or the rigid body displacement a first step consists in calculating the residual displacements [1]. The thermo-elastic contact is solved in a second step. Compared to a purely elastic analysis the thermal strains act to modify the surface displacements, cf. eq. (2a). Plasticity introduces also a residual displacement of each point of the surface, indeed modifying the contact geometry, cf. eq. (2b). For more details the reader may refer to [3].

$$u_{ij} = u^e_{ij} + u^t_{ij} \tag{2a}$$

$$h_{ij} \leftarrow h_{ij} + u^r_{ij} \tag{2b}$$

In eq. (2a) u_{ij} is the total displacement, u^e_{ij} the elastic one and u^t_{ij} the displacement induced by thermal strains [2,3]:

$$u^t(A) = \int_\Omega m \cdot T(M) \cdot \varepsilon^*_{3kk}(M,A) \cdot d\Omega \tag{3}$$

with $m=\alpha_t[E/(1-2\nu)]$, α_t being the thermal expansion coefficient. A is the current point, M the integration point, $T(M)$ the temperature increase at point M of volume Ω, and $\varepsilon^*_3(M,A)$ the elastic strain tensor at point M due to a unit normal load (i.e. along 3) applied at point A of the surface. In the case of a stationary surface source in steady-state regime, u^t becomes :

$$u^t(A) = \frac{\alpha_t(1+\nu)}{\pi} \cdot q ** \int_0^{+\infty} \left(G^T ** G^U\right) \cdot d\xi_3 \tag{4}$$

with $q=Q_f \times p$ the surface heat flux (W/m^2). $Q_f=\beta \times \mu_f \times V$ is the heat factor (m/s), with β the repartition factor ($0< \beta <1$), μ_f the friction coefficient, and V the sliding speed (m/s). G^T and G^U are Green's function [3].

The initial geometry h_{ij} is updated in eq. (2b) with u^r_{ij} the residual (surface) displacement. The last one yields from the plastic strain tensor:

$$u^r_{ij}(A) = 2\mu \int_{\Omega_p} \varepsilon^p_{ij}(M) \cdot \varepsilon^*_{3ij}(M,A)\, d\Omega \tag{5}$$

with A the current point, M the integration point, μ the Lamé coefficient, Ω_p the plastic volume (where $\varepsilon^P=0$), $\varepsilon^p(M)$ the tensor of plastic strain at point M.

The plastic strain increment $\delta\varepsilon^p$ is calculated by the Newton-Raphson with the return-mapping algorithm [5,6]. The surface displacement increment for each point of the surface is then calculated and added to the initial geometry, eq. (2b), until convergence. It is then possible to modify the applied load or to move one of the bodies relatively to the other.

3 APPLICATION TO THE PREDICTION OF RESIDUAL STRESSES DUE TO GRINDING

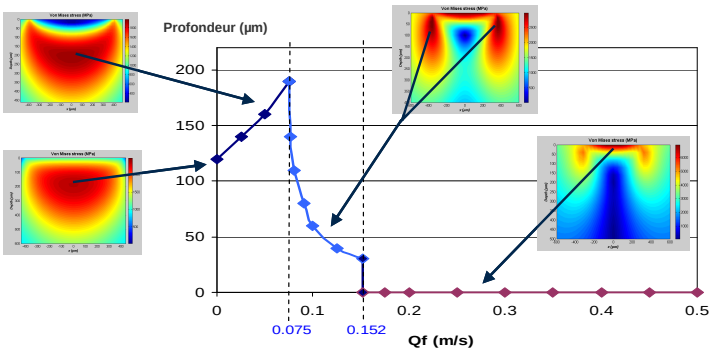

Fig. 1. Depth where the von Mises stress at the onset of yielding is found maximum, versus the heat factor Qf =µf.β.ΔU (stationary circular point contact).

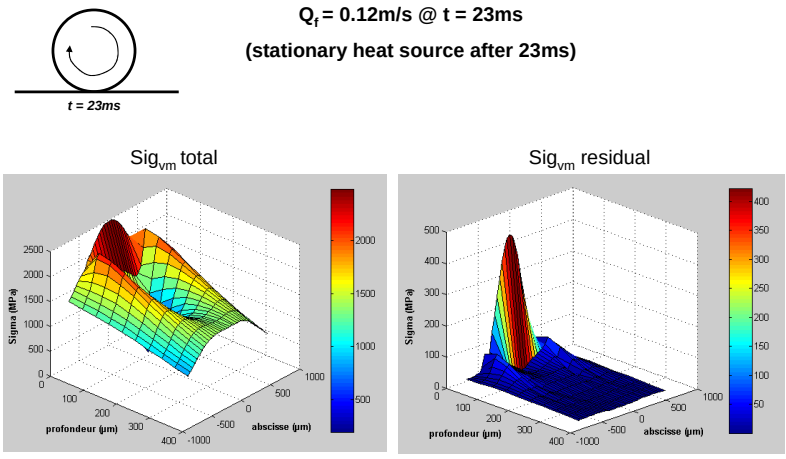

Fig. 2. Von Mises stress under loading (left) and after unloading (right) 23 ms after the beginning of the thermo-mechanical loading for a stationary circular point contact.

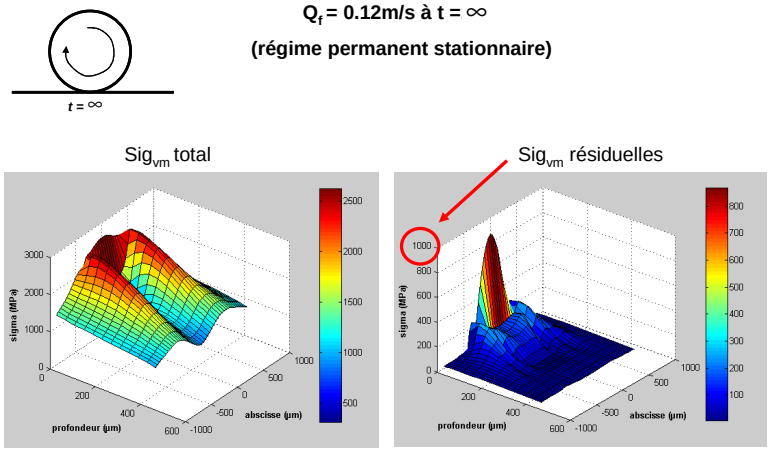

Fig. 3. Von Mises stress under loading (left) and after unloading (right) for a stationary sphere on flat contact under steady-state regime.

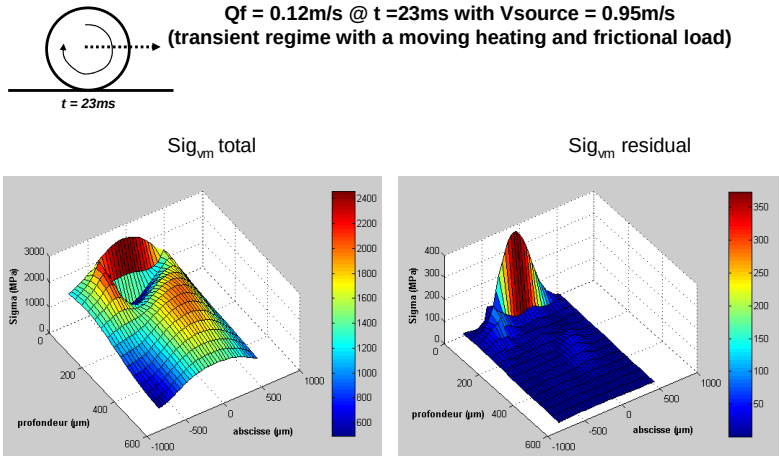

Fig. 4. Von Mises stress under loading (left) and after unloading (right) 23 ms after the beginning of the load/source movement (circular point contact).

A first example is given in Fig. 1 which illustrates the competition between thermal and mechanical effects. It concerns the contact between an adiabatic elastic sphere ($E=210\ GPa$, $\nu=0.3$) of diameter 15 mm in contact with an elastic-plastic flat in AISI 52100 steel of identical elastic properties and isotropic hardening behaviour described by the following Swift law: $\sigma_{VM}=B(C+\varepsilon^p)^n$ with $B=945\ MPa$, $C=20$ and $n=0.121$, ε^P being expressed in µ-strain. The thermal properties of AISI 52100 steel are: $K=50.2\ W/m.K$ and $\alpha_t=11.7\ \mu m/m.K$. The normal load is kept equal to the critical load at the onset of yielding, and the tangential effects are neglected. The contact is stationary and in steady-state regime which means that the heat source and the contact area are stationary, the observation time being infinite.

First it should be observed that the dissipation at the interface modifies significantly the subsurface stress distribution (under load). The increase of the heat factor from *0* to *0.5 m/s* seems first to produce an apparent decrease of the stress state below the

surface, then starts to push the maximal stress at the border of the contact, and finally produces a very high stressed area at the surface in the center of the contact. Note that a sliding speed of *50 m/s* along with a friction coefficient of *0.01* corresponds to a heat factor of *0.5 m/s*.

The heat factor Q_f is now assumed equal to *0.12 m/s* with a normal load of *150 daN*. Lets observe the stress state *23 ms* after the beginning of the thermo-mechanical loading. The von Mises stress fields under load and after unloading are given in Fig. 2. The same results are given in Fig. 3 when the observation time tends to infinite.

The stress fields under load and after unloading are given in Fig. 4 when the rotating tool is moving at a constant linear speed of *0.95 m/s*, after *23 ms*.

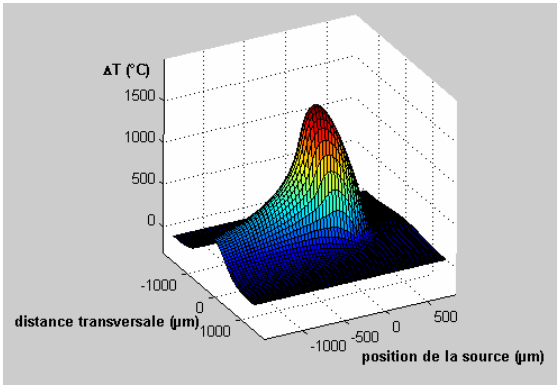

Fig. 5. Surface temperature rise after 23 ms, for Fig. 4.

The corresponding surface temperature distribution is given in Fig. 5. Note that the maximum temperature is higher than *1000°C*. However the normal load is here quite high and the contact area small. The same simulation with a cylindrical tool (instead of a spherical one) or a lower level of normal load should lead to temperature and stress distributions probably more realistic.

4 CONCLUSION

This first investigation highlights the potential of the semi-analytical method for the simulation of the grinding process. More work is needed, first to compare numerical results to experimental ones, second to include more physics in the model.

REFERENCES

1. Jacq C., Nélias D., Lormand G., Girodin D., 2002, "Development of a Three-Dimensional Semi-Analytical Elastic-Plastic Contact Code," *ASME J. Tribol.*, **124** (4), 653–667.
2. Liu S., Wang Q., 2001, "A Three-Dimensional Thermomechanical Model of Contact Between Non-Conforming Rough Surfaces," *ASME J. Tribol.*, **123**, 17–26.
3. Boucly V., Nélias D., Liu S., Wang Q.J., Keer L.M., 2005, "Contact Analyses for Bodies with Frictional Heating and Plastic Behavior," *ASME J. Tribol.*, **127** (2), 355-364.
4. Polonsky I.A., Keer L.M., 1999, "A Numerical Method for Solving Rough Contact Problems Based on the Multi-Level Multi-Summation and Conjugate Gradient Techniques," *Wear*, **231**, 206–219.
5. Fotiu P.A., Nemat-Nasser S., 1996, "A Universal Integration Algorithm for Rate-Dependant Elastoplasticity," *Comput. Struct.*, **59**, 1173–1184.
6. Nélias D., Boucly V., Brunet M., 2006, "Elastic-Plastic Contact between Rough Surfaces: Proposal for a Wear or Running-in Model," *ASME J. Tribol.*, **128** (2), 236–244.
7. Chiu Y.P., 1977, "On the Stress Field Due to Initial Strains in a Cuboid Surrounded by an Infinite Elastic Space," *ASME J. Appl. Mech.*, **44**, 587–590.
8. Chiu Y.P., 1978, "On the Stress Field and Surface Deformation in a Half-Space With a Cuboidal Zone in which Initial Strains Are Uniform," *ASME J. Appl. Mech.*, **45**, 302–306.
9. Gallego L., Nélias D., 2007, "Modeling of Fretting Wear under Gross Slip and Partial Slip Conditions," *ASME J. Tribol.*, **129** (3), 528-535.
10. Nélias D., Antaluca E., Boucly V., 2007, "Rolling of an Elastic Ellipsoid upon an Elastic-Plastic Flat". *ASME J. Tribol.*, **129** (4), 791-800.
11. Antaluca E., Nélias D., 2008, "Contact Fatigue Analysis of a Dented Surface in a Dry Elastic-Plastic Circular Point Contact". *Tribology Letters*, **29** (2), 139-153.
12. Warren A.W., Guo Y.B., 2005, "Fast Methods for Solving Rough Contact Problems: a Comparative Study," *Trib Trans.*, **48**, 436–441.
13. Hamdi H., Zahouani H., Bergheau J.-M., 2004, "Residual Stresses Computation in a Grinding Process," *J. Mat. Processing Techn.*, **147** (3), 277–285.
14. Boucly V., Nélias D., Green I., 2007, "Modeling of Rolling and Sliding Contact between Two Asperities". *ASME J. Tribol.*, **129** (2), 235-245.